

# An Efficient Localization Scheme With Velocity Prediction for Large-Scale Underwater Acoustic Sensor Networks

Yiran Wang<sup>ID</sup>, Shanshan Song<sup>ID</sup>, Member, IEEE, Xiaoxin Guo<sup>ID</sup>, Jun Liu<sup>ID</sup>, Member, IEEE,  
Qiang Ye<sup>ID</sup>, Senior Member, IEEE, and Jun-Hong Cui, Member, IEEE

**Abstract**—Localization is vital and fundamental for underwater acoustic sensor networks (UASNs), as it provides location information for UASNs to achieve various practical underwater tasks. Most existing localization methods assume small-scale scenarios without battery energy constraints, making it inapplicable to large-scale UASNs. In large-scale UASNs, localization suffers from the challenges of excessive energy consumption and large localization error because of harsh underwater conditions like node mobility and huge ranging errors. To this end, we propose an efficient localization scheme with velocity prediction (LSVP) to solve the above challenges for large-scale UASNs. LSVP considers node mobility, ranging errors, and energy balance in a unified framework, which is applicable to realistic and scalable UASNs. Specifically, we first design a Doppler-assisted velocity prediction (DVP) algorithm to decrease energy consumption, which can solve the excessive communications caused by node mobility under ocean currents. Then, a confidence-based iterative localization algorithm is proposed to decrease the localization error, which can reduce location uncertainty and error propagation caused by ranging errors. Extensive simulation results indicate that LSVP can achieve accurate velocity prediction and high precision localization for large-scale UASNs.

**Index Terms**—Error propagation, localization, mobility prediction, underwater acoustic sensor networks.

Manuscript received 18 June 2023; revised 31 July 2023; accepted 29 August 2023. Date of publication 4 September 2023; date of current version 6 February 2024. This work was supported in part by the National Natural Science Foundation of China under Grant 62101211 and Grant 61971206; in part by the National Key Research and Development Program of China under Grant 2021YFC2803000; in part by the Overseas Top Talents Program of Shenzhen under Grant KQTD2018041118495597; and in part by the Special Funds Program for Promoting Economic Development of Guangdong under Grant GDME-2018A002. (*Corresponding author: Shanshan Song*.)

Yiran Wang, Shanshan Song, and Xiaoxin Guo are with the Department of Computer Science and Technology, Jilin University, Changchun 130012, China (e-mail: wzr20@mails.jlu.edu.cn; songss@jlu.edu.cn; guoxx@jlu.edu.cn).

Jun Liu is with the School of Electronic and Information Engineering, Beihang University, Beijing 100191, China, and also with the Robotics Research Center, Peng Cheng Laboratory, Shenzhen 518055, China (e-mail: liujun2019@buaa.edu.cn).

Qiang Ye is with the Department of Computer Science, Memorial University of Newfoundland, St. John's, NL A1B 3X5, Canada (e-mail: qiangy@mun.ca).

Jun-Hong Cui is with the College of Computer Science and Technology, Jilin University, Changchun 130012, China, and also with the Shenzhen Ocean Information Technology, Industry Research Institute, Shenzhen 518055, China (e-mail: junhong\_cui@jlu.edu.cn).

Digital Object Identifier 10.1109/JIOT.2023.3311791

## I. INTRODUCTION

UNDERWATER acoustic sensor networks (UASNs) are emerging for their commercial and military value. UASNs helps to collect and transmit data for underwater environment monitoring, scientific exploitation, disaster prevention, and target detection [1]. The collected data (temperature, salinity, pressure, and current speed) needs location information to achieve the above missions. For instance, nodes cooperate sensing data with their locations to make detection relevant. Media access control [2] and geo-routing protocol [3] rely on location information to avoid collisions and find forwarding path. Therefore, localization is vital and fundamental for UASNs [4].

Localization is challenged by low channel bandwidth, long and variable propagation delay, Doppler effect, and energy limitation. So far, numerous schemes for localization have been proposed for UASNs. Some of these focus on the small-scale static scenarios (ten or less nodes) where the locations of all sensor nodes are fixed during the lifetime, since they are anchored by buoys [5], [6]. These schemes are able to calculate accurate locations but have limited coverage, which are not conducive to the network expansion. Driven by underwater applications, the scale of UASNs has continued to expand (dozens to hundreds of nodes). Therefore, various localization schemes for large-scale static scenarios have emerged [7], [8]. These schemes adopt an iterative strategy to improve the localization rate, that is, more nodes can calculate their locations during the mission process. However, the above methods are not suitable for practical scenarios where most sensor nodes are free-floating and drift with ocean currents (Fig. 1). Consequently, some algorithms for large-scale mobile scenarios have been proposed [9], [10]. Although the above localization schemes have achieved great results, we still face the following two challenges for large-scale mobile UASNs.

**Energy Constraints:** Underwater sensor nodes are constrained by energy as their battery capacity is limited. During the localization process, communication (tens to hundreds of watts) is the major factor in energy consumption, which is much higher than calculation (single watt or less) [11]. In UASNs, sensor nodes are continuously shifting as they are driven by the ocean current, so the localization algorithm updates their position information periodically by a high frequency of communication, which dramatically increases the

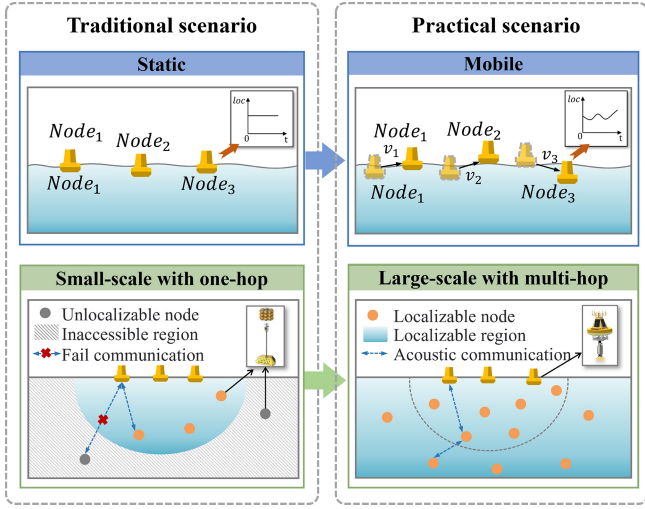


Fig. 1. Example to illustrate the distinction between two scenarios. Traditional methods assume a small-scale static scenario, while the present paper focuses on localization for a large-scale mobile scenario.

energy consumption and shorten nodes' lifetime. Therefore, how to reduce communication frequency to minimize energy consumption is the first challenge.

*Localization Error:* There are two main reasons for the large localization error in large-scale UASNs.

- 1) *Localization Uncertainty:* Sensor nodes usually receive many localization messages from different reference neighbors, and the time stamps carried by these messages are used for distance measurement. However, it is not proportional to the time of arrival (TOA) due to the dynamic sound velocity, which causes ranging errors. Under ranging errors, choosing different reference nodes leads to varying localization results, which introduce localization uncertainty.
- 2) *Error Propagation:* In large-scale UASNs, localization is an iterative process in which the localized nodes serve as pseudo-anchors to assist their neighbors in localizing. The pseudo-anchors localization error will propagate and accumulate to the later nodes. Therefore, how to reduce localization uncertainty and alleviate error propagation is the second challenge.

To this end, we propose an efficient localization scheme with velocity prediction (LSVP) mechanism for large-scale underwater acoustic sensor networks, which can provide real-time location with high accuracy and low energy consumption for each node. For the first challenge, we design a Doppler-assisted velocity prediction (DVP) algorithm. DVP uses historical velocity information to predict nodes' location, which decreases energy consumption by reducing communication frequency. DVP performs in two steps: 1) Doppler scaling factor estimation is used to obtain accurate historical velocity information for sensor nodes and 2) combining historical velocity information with semi-periodicity of the node mobility pattern, nodes can predict their velocity over a period of time and derive future location. To solve the second challenge, we design a confidence-based iterative localization (CIL) algorithm to improve localization accuracy. CIL implements high-accuracy localization in two steps: 1) the unknown node acquires the optimal reference node set for

localization by quantifying the geometric layout of different reference node set, and calculates its location and 2) then, node calculates a confidence value based on the result of localization and confidence information of reference nodes. Nodes with high confidence values are regarded as pseudo-anchors, which can broadcast their locations for iterative localization. Simulation results show that our scheme can reduce energy consumption and achieve high-precision localization. The main contributions are summarized as follows.

- 1) We study the challenges and propose an efficient LSVP mechanism for large-scale UASNs, which can prolong network lifetime (NL) while providing high-precision localization.
- 2) A DVP scheme, which can restrain energy consumption by reducing the communication frequency, is proposed for anchor nodes. DVP combines the Doppler factor estimation with the semi-periodicity of node mobility pattern to predict the locations of anchor nodes.
- 3) A CIL method is designed to reduce the localization error caused by localization uncertainty and error propagation. CIL helps to choose reference nodes which form a favorable geometric layout. Then, each localized node calculates its confidence value to assist iterative localization.
- 4) We conduct extensive simulations to evaluate the performance of our scheme. The results demonstrate that our scheme can improve the accuracy of localization and prolong the NL compared to the state-of-the-art approaches.

The remainder of this article is organized as follows. In Section II, we review the related work of localization in UASNs. In Section III, we present the preliminaries knowledge of LSVP. In Section IV, we describe LSVP in detail. Simulation results are provided in Section V. Finally, we conclude this article in Section VI.

## II. RELATED WORK

In recent years, researchers have proposed novel methods for UASNs localization. In most cases, localization methods are applied in particular scenarios. To meet the different requirements of the application, localization scenarios can be categorized into small-scale UASNs and large-scale UASNs.

### A. Small-Scale UASNs

Currently, most studies on localization for underwater sensor networks are mainly designed for static small-scale networks. Lee and Kim [12] proposed a range-free localization method with mobile beacon. Beacon nodes broadcast their location message periodically and other sensor nodes are located by passively receiving the beacon information. In this algorithm, sensor nodes first obtain a set of potential locations as candidate positions, and then calculate the location through the weighted mean of all the potential locations. In [13], an area localization scheme was proposed based on region division. In this scheme, anchor nodes partition the region into nonoverlapping areas by sending messages at different powers. Other nodes listen to anchor messages which carry an indicator of the transmit power and keep a list of the anchors and their

corresponding power levels. Then, they send the information to the sink node which determines the location of sensor nodes based on known information.

The above range-free localization methods are coarse-grained localization techniques that cannot provide precise location information. Cheng et al. [14] presented a silent positioning scheme termed UPS. UPS detects the time difference of arrival to obtain the range differences between unknown nodes and four anchor nodes. UPS employs four anchors to send beacon signals in sequence and then the unknown node estimates location using anchor messages and the range differences according to the trilateration. In [15] and [16], a USP localization framework was proposed for 3-D UWSNs. In USP, sensor nodes are equipped with underwater pressure sensors which can transform 3-D underwater localization problem into 2-D via projection technique. USP considers the stratification effect of the actual underwater environment and improves localization performance through bilateral iteration.

### B. Large-Scale UASNs

In general, the area for many underwater surveillance applications is vast. Therefore, it is essential to utilize large-scale underwater networks to carry out these applications. In large-scale underwater networks, the accuracy of localization and energy consumption of communication make it more challenging. Zhou et al. [7] proposed a distributed localization scheme, which integrates a 3-D Euclidean distance estimation with a recursive location estimation method to realize localization in the whole network. Zhou et al. [17] proposed an asymmetrical round-trip-based localization algorithm termed ARTL. ARTL uses only one pair of message exchange and passively listen to the beacons for information which achieve accurate and energy efficient node localization in large-scale underwater networks. Su et al. [8] proposed a mobile-beacon-based iterative localization algorithm for large-scale underwater networks which have a higher proportion of localized nodes and reduce the localization error above the whole networks. MBIL uses mobile beacon nodes to localize adjacent sensor nodes which will calculate their confidence value to assist the unknown nodes in localization.

On this basis, many localization algorithms for mobile nodes have been proposed to accommodate the real marine environments. Zhou et al. [9] proposed an SLMP scheme for large-scale mobile underwater sensor networks. SLMP can estimate the future location of sensor nodes by utilizing the predictable mobility patterns of underwater objects, which will reduce the energy consumption generated by communication significantly. Then, the algorithm adopts a hierarchical iterative localization approach which achieves a high proportion of localized nodes. In [18], to reduce the prediction error of the SLMP, Chen et al. used a multistep Levinson Durbin algorithm to improve the accuracy of the estimation location. In [10], a node dynamic localization and prediction algorithm are proposed. A new node mobility model is improved based on the actual marine environment. A frequency-based prediction algorithm for anchor nodes and a deep information-based weighted fusion method for ordinary nodes are well

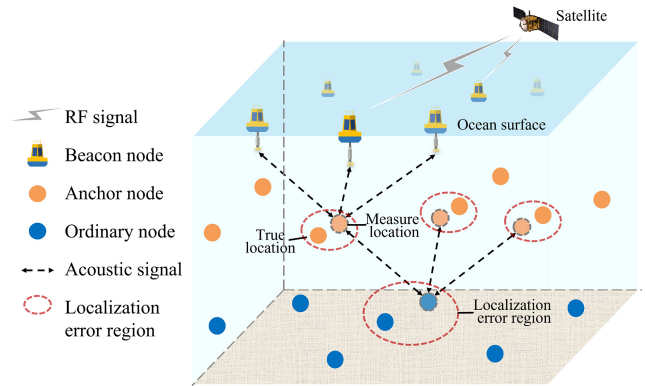


Fig. 2. Scenario of the UASNs. Few beacon nodes are deployed sparsely on the ocean surface. The red dotted circle marks the localization error region. Nodes farther from the beacon nodes have larger localization error region.

designed. The above mobile localization techniques all work for dense networks because they are all based on spatial correlation.

## III. PRELIMINARIES

### A. Network Scenario

To accomplish localization for large-scale UASNs, we consider a general scenario, as shown in Fig. 2. The network scenario comprises satellite, beacon nodes, anchor nodes, and ordinary nodes.

- 1) *Satellite*: Satellite can provide timely location information for beacon nodes via radio-frequency (RF) communication.
- 2) *Beacon Nodes*: Beacon nodes equipped with GPS devices are float on the water surface sparsely. They communicate with satellites to obtain real-time location. They broadcast their location periodically to assist underwater nodes (anchor nodes and ordinary nodes) in localization.
- 3) *Anchor Nodes*: Anchor nodes can make direct contact with the beacon nodes. Anchor nodes can correct locations based on range information while communicating with multiple beacons. They can predict locations using historical data when they are not communicating with beacon nodes. Then, anchor nodes broadcast their information to assist ordinary nodes in localization.
- 4) *Ordinary Nodes*: Ordinary nodes cannot communicate with beacon nodes directly, but they can connect to their one-hop neighbors. Ordinary nodes can achieve self-localize by connecting with the located anchor nodes or ordinary nodes.

### B. Network Assumptions

In the above network scenario, the localization assumptions are itemized as follows.

- 1) The whole scenario consists of a few beacon nodes and a large number of underwater nodes (anchor nodes and ordinary nodes).
- 2) Beacon nodes are powered by solar energy, so there is no energy consumption limit. Underwater sensor nodes are powered by batteries. When a node's battery is below the threshold, it will no longer communicate.

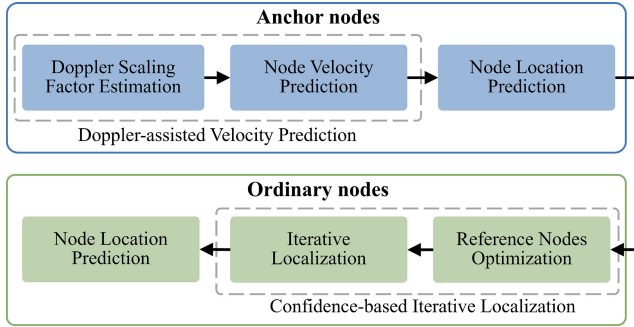


Fig. 3. Framework of LSVP. LSVP includes two subprocesses: anchor nodes localization and ordinary node localization.

- 3) All sensor nodes are assumed to be properly synchronized, so the distance between two nodes can be estimated through the TOA.
- 4) All sensor nodes are equipped with underwater pressure sensors to obtain depth information, which can simplifies the complex 3-D problems into 2-D problems. Therefore, only the horizontal coordinates need to be calculated for localization. In this manner, each sensor node only needs the range information from three reference nodes to achieve self-localization.

### C. Overview of LSVP

In our scenario, each sensor node is required to obtain its location periodically. In the initial phase, only beacon nodes know their locations through GPS. Based on the limited number of known location nodes, unknown nodes can calculate their locations through an iterative localization mechanism.

To achieve efficient large-scale localization in UASNs, LSVP divides the whole localization process into two subprocesses: 1) anchor nodes localization and 2) ordinary nodes localization. The whole framework of LSVP is shown in Fig. 3. In Fig. 3, two dotted boxes solve two key issues for LSVP: 1) reducing communication consumption and 2) improving localization accuracy.

The dotted box above represents the DVP algorithm, which reduces communication consumption. In DVP, each anchor node can achieve Doppler scaling factor estimation with the assistance of beacon nodes to obtain its velocity. Then, a series velocity refined by the Kalman filter can provide high-precision velocity information for node velocity prediction. According to DVP and previous location, node can achieve location prediction. Benefiting from DVP, beacon nodes do not need to broadcast their message in every localization period, which reduces the frequency of communication.

The dotted box below represents the CIL algorithm, which can improve localization accuracy. In CIL, ordinary nodes first execute reference nodes optimization strategy to reduce localization uncertainty, after receiving at least three reference nodes. After one ordinary node completes self-localization, it will calculate a confidence value to determine whether it can assist the rest nodes in iterative localization. Benefiting from CIL, unknown node chooses a favorable reference node set to reduce localization uncertainty, and uses high-confidence reference nodes to alleviate error propagation. Finally, an

TABLE I  
NOTATION LIST

Notation	Definition
$T$	Localization period
$T_w$	Velocity prediction unit
$p_i = (x_i, y_i)$	Real location vector of node $i$
$\hat{p}_i = (\hat{x}_i, \hat{y}_i)$	Estimation location vector of node $i$
$d(p_i, p_j)$	Euclidean distance between node $i$ and node $j$
$\hat{v}_{ij}$	The relative velocity between node $i$ and node $j$
$v_i$	The velocity of node $i$
$\eta_i$	Confidence value of node $i$
$\psi$	Reference node set
$Q$	Quality of self-localization
$\xi$	Residual energy of node $i$

ordinary node can deduce its mobility pattern from nearby nodes, which can achieve node location prediction.

The notations in this article are summarized in Table I.

### IV. DESCRIPTION OF LOCALIZATION SCHEME

LSVP is designed to achieve low-energy and high-accuracy localization performance for large-scale UASNs. To limit energy consumption, each sensor node uses a velocity prediction mechanism to calculate its future location. To improve localization accuracy, an iterative localization mechanism is employed to reduce localization uncertainty and alleviate error propagation. LSVP considers different capabilities of sensor nodes and divides the entire localization process into anchor nodes localization and ordinary nodes localization.

#### A. Anchor Nodes Localization

Anchor nodes can obtain their locations at any time because they communicate with beacon nodes directly. However, frequent communication will lead to enormous energy consumption. Therefore, a DVP algorithm is designed to limit energy consumption, in which anchor node can predict its future velocity based on the historical and achieve node location prediction.

1) *Doppler-Assisted Velocity Prediction*: In this stage, each anchor node can achieve Doppler scaling factor estimation with the assistance of beacon nodes to obtain its velocity. Then, a series velocity refined by the Kalman filter can provide high-precision velocity information for node velocity prediction.

*Doppler Scaling Factor Estimation*: We obtain the relative velocity by Doppler scaling factor estimation. The Doppler scaling factor estimation is completed by the cooperation of a special preamble at the sender and a multibranch parallel auto-correlators at the receiver [19], [20].

On the sender side, the structure of a localization packet with the special preamble is shown in Fig. 4. The preamble consists of a cyclic prefix and two identical waveforms. And each data field is explained as follows.

- 1) *Node Id*: A symbol which exclusively identifies the sender.
- 2) *Location*: The current location of the sender.

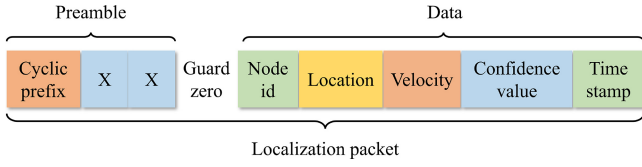


Fig. 4. Structure of a localization packet of acoustic communication.

- 3) *Velocity*: Current and a series predicted velocity of the sender.
- 4) *Confidence Value*: The confidence value of the sender, which is used to indicate the accuracy of the location estimation. It is used to assist the later iterative localization.
- 5) *Time Stamp*: Sending time of this packet, which is obtained at MAC layer. This timestamp can be used for distance estimation by TOA.

Defining  $x(t)$  as the baseband signal, the sender sends a baseband waveform with repetition pattern as

$$x(t) = x(t + T_0), \quad -T_{cp} \leq t \leq T_0 \quad (1)$$

where  $T_0$  and  $T_{cp}$  are the time duration of the waveform and the cyclic prefix. The repetition pattern persists at the receiver side even after multipath propagation and the received baseband signal  $y(t)$  is expressed as

$$y(t) = e^{-2\pi f_c T_0 \frac{a}{a+1}} y\left(t + \frac{T_0}{1+a}\right) \quad (2)$$

where  $t \in [-(T_{cp} - \tau_{\max}/1+a), (T_0/1+a)]$ ,  $f_c$  denotes the carrier frequency,  $a$  is the Doppler scaling factor we want to acquire, and  $\tau_{\max}$  is the channel multipath delay spread. Due to the complex multipath acoustic channel, the receiver does not know the period and the waveform. We need to infer the repetition period from the receiving signal and then obtain the Doppler scale.

On the receiver, the discrete-time expression of the baseband signal  $y(t)$  is sampled at multiple of the system bandwidth  $t_s$ , as

$$y[n] = y(t)|_{t=nt_s}, \quad t_s = \frac{1}{\lambda B} \quad (3)$$

where the sampling factor  $\lambda$  is an integer, and  $B$  is the signal frequency bandwidth. In order to estimate the Doppler scaling factor, the receiver uses a set of auto-correlators to obtain the periodic characteristic of the received preamble, as shown in Fig. 5. Each branch can match to a certain period  $P_l$ . The receiver performs the following steps.

- 1) First, each branch calculates a correlation metric  $|M|$  with value of the window size  $P_l$  as

$$M(P_l, d) = \frac{\sum_{i=d}^{d+P_l-1} y[i]y[i+P_l]}{\sqrt{\sum_{i=d}^{d+P_l-1} |y[i]|^2 \cdot \sum_{i=d}^{d+P_l-1} |y[i+P_l]|^2}} \quad (4)$$

where  $d$  is the index of auto-correlation outputs and  $l = 1, 2, \dots, L$ .

- 2) Then, if the value of the correlation metric of any branch is larger than the preset threshold  $\delta_{th}$ , the receiver will

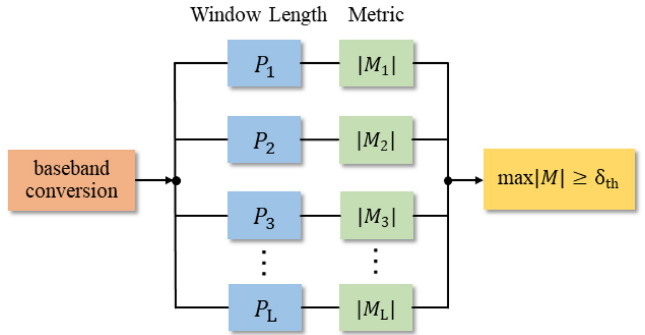


Fig. 5. Structure of multibranch parallel auto-correlators.

announce that it detects a useful signal as

$$\max_l |M(P_l, d)| > \delta_{th}, \quad \delta_{th} \in [0, 1]. \quad (5)$$

- 3) In the end, the branch with maximum correlation metric can be seen as having the best matching performance with the repetition length. So the Doppler scaling factor can be estimated as

$$\hat{a} = \frac{\frac{T_0}{\lambda B} - \hat{P}}{\hat{P}}, \quad \hat{P} = \arg \max_{P_l} |M(P_l, d)|. \quad (6)$$

Using the Doppler scaling factor, we can estimate the relative moving velocities between the sender and the receiver as

$$\hat{v} = c\hat{a} \quad (7)$$

where  $c$  is the propagation speed of acoustic signal in water.

To estimate the velocity of node  $i$ , there must be at least three relative velocities of reference nodes. When node  $i$  receives a localization packet from reference node  $j$ , it can extract location information  $p_j = (x_j, y_j)$  and velocity information  $v_j = (v_j^x, v_j^y)$  from the data part and calculate a relative velocity  $\hat{v}_{ij}$  through (7). Once node  $i$  receives localization packet from three reference nodes, it can estimate the location  $p_i$  by trilateration, and then calculate the velocity  $v_i$  by

$$\hat{v}_{ij} = \frac{(x_j - x_i - \Delta t v_j^x) \cdot v_i^x + (y_j - y_i - \Delta t v_j^y) \cdot v_i^y}{(x_j - x_i - \Delta t v_j^x)^2 + (y_j - y_i - \Delta t v_j^y)^2} \quad (8)$$

where  $j$  is from 1 to 3, and  $\Delta t$  indicates the duration of propagation. The whole process of Doppler-assisted velocity estimation is shown in Algorithm 1.

Since multiple consecutive communication occurred during velocity estimation stage, the estimation can be further refined by the Kalman Filter to obtain serial high-precision velocity data as the basis for the velocity prediction.

*Node Velocity Prediction*: Underwater objects are usually moving with ocean current continuously. The moving pattern has semi-periodical characteristics [21]. So the historical velocity information estimated by the Doppler scaling factor with the Kalman filter can be used to predict the future velocity of sensor nodes.

The mobility pattern of sensor nodes in the seashore environment is a similar waveform to the voice signal, which can be approximated by the all-pole model. Linear prediction

**Algorithm 1:** Doppler-Assisted Velocity Estimation

```

Input: The location of Node  $i$  as  $p_i$ 
Output: The velocity of Node  $i$  as  $v_i$ 
1 Beacon nodes broadcast localization packet for a period
   of time;
2 Wait for the localization packet from neighbors;
3  $k = 1$ ;
4 while  $k \leq 3$  do
5   Receive node  $j$ 's packet;
6   Save the location  $p_j$  and velocity  $v_j$  of node  $j$ 
      through the data part of the localization packet;
7   Calculate the relative velocity between node  $i$  and
      node  $j$  through Equation (7) as  $\hat{v}_{ij}$ ;
8    $k = k + 1$ ;
9 end
10 Calculate the velocity of node  $i$  through Equation (8) as
     $v_i$ ;
11 return  $v_i$ ;

```

algorithms are a common solution to the above prediction problem [9]. So we adopt a multistep Levinson–Durbin algorithm to predict the mobility of sensor nodes [22].

We divide time into multiple prediction units of fixed length. For ease of presentation, a single prediction unit is denoted as  $T_w = k \times T$ , where  $k$  is an integer and  $T$  is the localization period. We use velocity vector  $V = [v_{n+1}, v_{n+2}, \dots, v_{n+h}, \dots, v_{n+k}]$  to represent nodes mobility pattern in the prediction window, where  $v_{n+h}$  denotes the average velocity in the  $(n+h)$ th period and  $h$  represents the  $h$ th future state to be predicted. In multistep Levinson–Durbin algorithm, the best linear predictor of  $v_{n+h}$  given  $[v_{n+1-p}, \dots, v_{n-1}, v_n]$  can be expressed as follows:

$$v_{n+h}(p) = \sum_{j=1}^p a_p(j) v_{n+1-j} \quad (9)$$

where  $p$  is the length of the prediction steps, and  $a_p(j)$  represents the coefficient of  $v_{n+1-j}$ .

So far, the DVP algorithm has been introduced.

2) *Node Location Prediction:* In the prediction unit, beacon nodes stop providing location information to reduce energy consumption, and the anchor nodes need to calculate their location as

$$(x_{i,n+t}, y_{i,n+t}) = (x_{i,n}, y_{i,n}) + \sum_{m=n}^{n+t-1} T \times v_m \quad (10)$$

where  $t = 1, 2, \dots, k$ ,  $(x_{i,n}, y_{i,n})$  is the measurement location of node  $i$  in period  $n$  and  $v_m$  is the prediction velocity obtained from (9).

In the previous part, anchor nodes can predict their location based on the historical measurement information from multiple beacon nodes.

### B. Ordinary Nodes Localization

There are still many ordinary nodes need to be located in the network after anchor nodes localization. Since ordinary

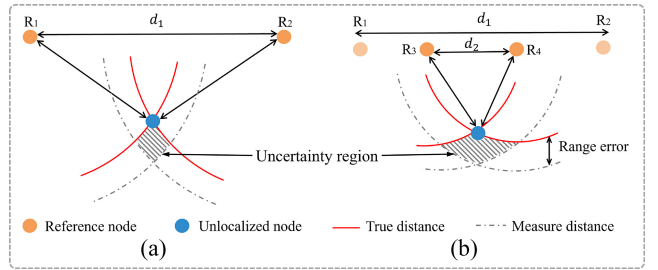


Fig. 6. Geometric relationship's influence on localization accuracy. (a) Localization uncertainty caused by geometric layout. (b) Localization uncertainty caused by worse geometric layout. The solid lines show the true distance between the unknown node and reference node, the dotted lines are the measurement distance. And the overlap region shows the localization uncertainty.

nodes cannot communicate with beacon nodes directly, they have to rely on the located nodes for localization. Therefore, we propose a CIL algorithm for ordinary nodes. CIL can improve localization accuracy by reducing localization uncertainty and alleviating error propagation. Based on CIL, if an ordinary node does not receive information packet during the localization period, it can use the spatial correlation model to predict the mobile characteristic and then deduce its location.

1) *Confidence-Based Iterative Localization:* In iterative localization stage, the ordinary node first selects the appropriate reference nodes to estimate its location. Then, it will assess the confidence value, which reflects the location error of reference nodes, quality of self-localization, and residual energy. The confidence value determines whether an ordinary node can be regarded as a pseudo-reference node to assist the rest nodes in iterative localization.

*Reference Nodes Optimization:* The geometric relationship between reference nodes and unknown node will significantly affect the accuracy of location estimation [23]. The distribution of reference nodes with poor geometric relationship will cause large uncertainty and further result in worse location estimation. Fig. 6 shows an example that may occur in the actual scenario. There are three reference nodes  $R_1$ ,  $R_2$ , and  $R_3$ , and  $U$  is the unknown node, the solid lines show the true distance between the unknown node and reference nodes while the dotted lines are the measurement distance. The gap between these two kinds of lines is the ranging error which is assumed to be independent and identical. The overlap region represents the possible location of the unknown node, which can also be regarded as the localization uncertainty region. A smaller overlap region means lower localization uncertainty. It is obvious that the localization uncertainty in Fig. 6(a) is larger than in Fig. 6(b).

Geometric dilution of precision (GDOP) can be used to evaluate the geometric relationship effect to the accuracy of location estimation [24], [25]. A smaller GDOP value means less localization uncertainty. Therefore, it is necessary to choose the appropriate combination of reference nodes according to the geometric relationship to improve the accuracy of location estimation.

The underwater acoustic signal is used for the TOA measurement in this article. For ease of presentation, the location

vector of unknown node  $i$  is denoted as  $p_i = (x_i, y_i)$ , and  $p_n = (x_n, y_n)$  is the location vector of reference node  $n$ , where  $n$  is from 1 to 3. The measurement distance is denoted as

$$\varphi_n = ct_n \quad (11)$$

where  $t_n$  is the measurement time between unknown node  $i$  and reference node  $n$ , and  $c$  is the propagation speed of acoustic signal in water. So the measurement relationship can be represented as

$$\varphi_n = \sqrt{(x_i - x_n)^2 + (y_i - y_n)^2} + \omega \quad (12)$$

where  $\omega$  is the measurement noise. When the unknown node received at least three localization information, node uses the Least Square Method to acquire an initial location estimate  $\hat{p}_i = (\hat{x}_i, \hat{y}_i)$ . Defining  $\hat{\varphi}_n$  as  $\varphi_n$  at  $(\hat{x}_i, \hat{y}_i)$ , the first-order Taylor expansion for (12) at  $\hat{p}_i = (\hat{x}_i, \hat{y}_i)$  neglecting the higher order terms can be expressed as

$$\Delta\varphi_n = \varphi_n - \hat{\varphi}_n = \frac{\partial\varphi_n}{\partial x_i} \Delta x + \frac{\partial\varphi_n}{\partial y_i} \Delta y - \omega \quad (13)$$

where

$$\frac{\partial\varphi_n}{\partial x_i} \Big|_{p=\hat{p}} = \frac{\hat{x}_i - x_n}{l_n}, \quad \frac{\partial\varphi_n}{\partial y_i} \Big|_{p=\hat{p}} = \frac{\hat{y}_i - y_n}{l_n} \quad (14)$$

with

$$l_n = \sqrt{(\hat{x}_i - x_n)^2 + (\hat{y}_i - y_n)^2}. \quad (15)$$

The above formula can be stacked into a vector matrix formulation as

$$\underbrace{\begin{bmatrix} \Delta\varphi_1 \\ \Delta\varphi_2 \\ \Delta\varphi_3 \end{bmatrix}}_{:=\Delta\varphi} \approx \underbrace{\begin{bmatrix} \frac{\hat{x}_i - x_1}{l_1} & \frac{\hat{y}_i - y_1}{l_1} & 1 \\ \frac{\hat{x}_i - x_2}{l_2} & \frac{\hat{y}_i - y_2}{l_2} & 1 \\ \frac{\hat{x}_i - x_3}{l_3} & \frac{\hat{y}_i - y_3}{l_3} & 1 \end{bmatrix}}_{:=H} \cdot \underbrace{\begin{bmatrix} \Delta x \\ \Delta y \\ \omega \end{bmatrix}}_{:=\Delta X} \quad (16)$$

so the GDOP value  $G$  can be represented as

$$G = \sqrt{\text{trace}(H^T H)^{-1}}. \quad (17)$$

Above all, a combination with lower  $G$  value indicates better location estimation, which should be selected with higher priority level. When the unknown node receives more than three reference nodes' localization packets, the  $G$  value is calculated for any combination of three reference nodes. There will be  $C_N^3$  strategies to select the reference nodes. We calculate  $G$  for other node and obtain the mean for each combination. The combination acquiring the smallest  $G$  value is selected as the reference set. Using this reference set, we can estimate the final localization of the unknown node.

**Iterative Localization:** In our typical localization scenario, beacon nodes can only locate their adjacent nodes. To locate the remaining nodes, we propose an iterative localization method for global localization to obtain higher localization rate. When a sensor node has obtained its position, it needs to broadcast the message with its information to assist other nodes in localization. In this article, the confidence value  $\eta$  is

used to evaluate the reliability of the located node as a new reference node which reflects the quality of self-localization, location error of reference nodes, and residual energy.

*a) Quality of self-localization:* Different geometric distributions of reference nodes will bring different localization accuracy, and metric  $Q$  is proposed to quantify the effect of reference node selections on localization.  $Q$  can filter out the poor localization measurement with great uncertainty.

For notational convenience, the real location vector of node  $i$  is denoted as  $p_i$ , and  $\hat{p}_i$  is the estimation location of node  $i$ .  $d(p_i, p_j)$  represents the Euclidean distance corresponding to the node pairs  $p_i$  and  $p_j$ . Assume that the relative distance  $d(p_i, p_j)$  obeys some probability distribution, which can be expressed as probability density function  $f_{p_i, p_j}(s)$ , where  $s$  denotes the relative distance. In the scenario, the probability that any point  $p$  being the localization solution of reference node set  $\Psi$  is indicated by

$$f_\Psi(p) = \prod_{j=1}^3 f_{p_i, p_j}(d(p, p_j)). \quad (18)$$

Define  $O(p, r)$  as a circular area with  $p$  as the center and  $r$  as the radius. The quality of self-localization  $Q$  is defined as

$$Q_\Psi = \Pr(\hat{p}_i \in O(p_i, r)) \quad (19)$$

where  $r$  represents the value corresponding to different localization accuracy requirements. A large  $Q$  shows that the estimation location  $\hat{p}_i$  is close to the real location  $p_i$  with high probability. To calculate  $Q$ , the probability density needs to be integrated as

$$Q_\Psi = \int_p f_\Psi(p) dp, p \in O(\hat{p}_i, r) \quad (20)$$

which can be approximated by the light-weighted sampling method [26].

*b) Location error propagation:* In the iterative localization procedure, the location error is usually transmitted and accumulated. The localization error of current node is not only related to its quality of self-localization but also related to the location error of its reference nodes [27]. In this article, the error propagation of the reference nodes is taken into account. The confidence value  $\eta_i$  of node  $i$  based on reference node set  $\Psi$  is denoted as

$$\eta_i = Q_\Psi \times \prod_{j=1}^3 \eta_j \quad (21)$$

where  $\eta_j$  is the confidence value of node  $j$  in set  $\Psi$ .

The confidence value reflects how much we can rely on the localization result of node  $i$ . When the reference nodes have low confidence, the confidence value  $\eta_i$  will not be high. In the same way, if the reference nodes have high confidence, the confidence value  $\eta_i$  depends on the quality of localization. Initially, the confidence value of node  $i$  is assigned the value as

$$\eta_i = \begin{cases} 1, & \text{Beacon node} \\ 0, & \text{Otherwise.} \end{cases} \quad (22)$$

**Algorithm 2:** CIL

---

```

1 Initialization:  $\eta = 1$  for beacon nodes,  $\eta = 0$  for other
nodes;
2 Beacon nodes broadcast localization packet;
3  $k = 1$ ;
4 while  $p_i$  is unknown node do
5 | Wait for the localization packet from neighbors;
6 | if reference nodes  $\geq 3$  then
7 | | Choose the reference node set with highest  $G$ ;
8 | | Calculate the confidence value  $\eta_i$ ;
9 | | if  $\eta_i \geq \eta_{\min}$  then
10 | | |  $p_i$  becomes a pseudo-reference node;
11 | | |  $p_i$  broadcast localization packet;
12 | | else
13 | | |  $p_i$  stay silent;
14 | | end
15 | end
16 |  $k = k + 1$ ;
17 end

```

---

In iterative localization, the calculation of the confidence value is associated with the localization estimation, so the confidence value can be calculated after obtaining the reference information and self-localization.

c) *Residual energy*: To balance the energy consumption and prolong the NL, it is necessary to consider the residual energy  $\xi$  of nodes. Nodes with high residual energy should be considered as reference nodes and broadcast their localization messages. Nodes with low residual energy should stay silent.  $\xi_{\text{init}}$  represents the initial energy of node, so the ratio of  $\xi$  and  $\xi_{\text{init}}$  cannot be less than the threshold  $\xi_{\min}$ .

Therefore, the confidence value  $\eta_i$  is defined as

$$\eta_i = \begin{cases} 1, & \text{Beacon node} \\ 0, & \xi / \xi_{\text{init}} < \xi_{\min} \\ Q_\psi \times \prod_{j=1}^3 \eta_j, & \xi / \xi_{\text{init}} \geq \xi_{\min} \end{cases} \quad (23)$$

where  $\eta_{\min}$  is the confidence threshold. This means the CIL algorithm first restricts the communication of nodes with less residual energy to balance the energy consumption of the network. When the residual energy of the node  $i$  is sufficient, the localization error is further considered. So the confidence value of node  $i$  is jointly determined by the confidence value of its reference nodes and the quality of self-localization. If the confidence value is lower than the threshold  $\eta_{\min}$ , it implies that the localization error of node  $i$  is too large. When  $\eta_i \geq \eta_{\min}$ , node  $i$  can serve as a pseudo-reference node and broadcast its location information.

The whole process of CIL is illustrated in Algorithm 2.

2) *Node Location Prediction*: Ordinary nodes use the spatial correlation of underwater objects to predict the mobility pattern. Spatial correlation states that the moving pattern of one object is closely related to the motion of surrounding objects [21]. So we can infer the velocity of ordinary node

TABLE II  
PARAMETER SETTING

Parameter	Values
$k_1, k_2$	$N(\pi, 0.1\pi)$
$k_3$	$N(2\pi, 0.2\pi)$
$k_4, k_5, v$	$N(1, 0.1)$
$\lambda$	$N(3, 0.3)$
Transmission range $R_t$	$0.8 \leq R_t \leq 1.8(\text{km})$
Number of beacon nodes	10
Number of ordinary nodes	$80 \leq n \leq 120$
Single communication energy consumption $E_t$	12W
Sound speed $c$	1500m/s

$v_i$  from the velocity of adjacent nodes  $v_j$  as

$$v_i^x = \sum_{j=1}^m \tau_{ij} v_j^x, \quad v_i^y = \sum_{j=1}^m \tau_{ij} v_j^y \quad (24)$$

with:

$$\tau_{ij} = \frac{\frac{1}{d(p_i, p_j)}}{\sum_{j=1}^m \frac{1}{d(p_i, p_j)}} \quad (25)$$

where  $\tau_{ij}$  is the interpolation coefficients and  $m$  is the number of neighbors. Thus, the location can be calculated as

$$(x_{i,t+1}, y_{i,t+1}) = (x_{i,t}, y_{i,t}) + T \times v_i \quad (26)$$

where  $(x_{i,t}, y_{i,t})$  denotes the location of node  $i$  in period  $t$  and  $v_i$  is the estimated velocity of node  $i$  in period  $t$ .

## V. SIMULATION RESULTS

In this section, we will evaluate the performance of the algorithm through simulations.

### A. Simulation Settings

Multiple scenarios are used to assess the performance of the algorithm. Ten beacon nodes are distributed in different scenarios with different geometric deployment as triangle, grid, and random layout. In the above three scenarios, 120 underwater sensor nodes are randomly distributed in the monitoring area of  $5 \text{ km} \times 5 \text{ km} \times 3 \text{ km}$ . Referring to the existing underwater distance measurement technologies [28], the ranging error follows normal distribution with real distance as mean values and standard deviation to be 0.02 of distance. The whole simulation lasts for 1000 s, the localization period  $T$  is 1 s. The amount of velocity prediction data is 20.

We use the kinematic model, which is commonly used in the underwater environments, as the node mobility pattern. The moving speed of underwater objects in the kinematical model can be approximated as

$$\begin{cases} V_x = k_1 \lambda v \sin k_2 x \cos k_3 y + k_1 \lambda \cos 2k_1 t + k_4 \\ V_y = -\lambda \cos k_2 x \sin k_3 y + k_5 \end{cases} \quad (27)$$

Some relevant parameter settings are shown in Table II.

We compare our LSVF algorithm with the classical SLMP [9] and ULES [29] algorithm. Both SLMP and ULES are applicable localization algorithms for large-scale UASNs. SLMP uses mobility prediction to estimate locations and further improves the localization coverage rate by iteration. But

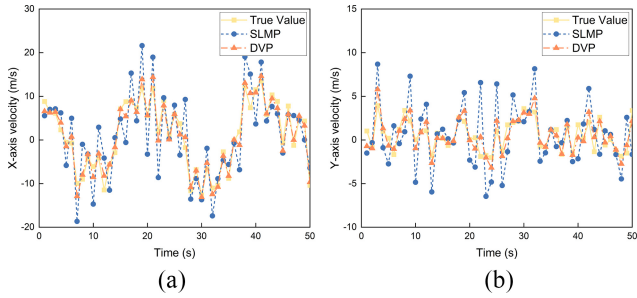


Fig. 7. Comparison of velocity estimation. (a) X-axis velocity prediction. (b) Y-axis velocity prediction.

have no concerns about the error propagation and the geometric relationship of reference nodes. ULES uses the reliability of each localized node for iteration and chooses high-reliability reference nodes for underwater localization without considering the energy consumption of the whole network. The performance of the algorithms is evaluated based on the average localization error (ALE) and the NL. The ALE can reflect the localization accuracy of the overall network nodes, formulated as

$$\text{ALE} = \frac{\sum_{i=1}^N \sqrt{(\hat{x}_i - x_i)^2 + (\hat{y}_i - y_i)^2}}{N \times R_t} \quad (28)$$

where  $N$  represents the number of all sensor nodes in the simulation scene. And the NL reflects the energy consumption of sensor nodes and is evaluated by the proportion of the alive sensors in the whole network, which can be calculated as

$$\text{NL} = \frac{N_a}{N} \quad (29)$$

where  $N_a$  is the number of alive sensor nodes in the network.

## B. Results Analysis

1) *Results of Velocity Estimation:* First, the anchor nodes need to collect continuous historical velocity information with high accuracy by communicating with the beacon nodes. We chose one of the anchor nodes to evaluate the effectiveness of the velocity estimation algorithm. We compare the DVP algorithm in this article and the location-based velocity estimation algorithm in SLMP. The true velocity in  $X(Y)$ -axis is recorded as the True Value. We choose the velocity estimation results during 50 s for presentation shown in Fig. 7. In Figs. 7(a) and (b), it can be seen that our method is closer to the true velocity which means a high accuracy on both  $X$ -axis and  $Y$ -axis than SLMP.

It is because the SLMP algorithm estimates velocity only depending on the location information. If nodes have low localization accuracy, they will cause a huge error in velocity estimation. In this article, the velocity estimation algorithm combines historical velocity information with observation information by the Kalman filter, which optimizes the velocity estimation. DVP can obtain high-precision velocity data as the basis for the velocity prediction.

2) *Results of Velocity Prediction:* Based on the historical data accumulated in the velocity estimation stage, anchor

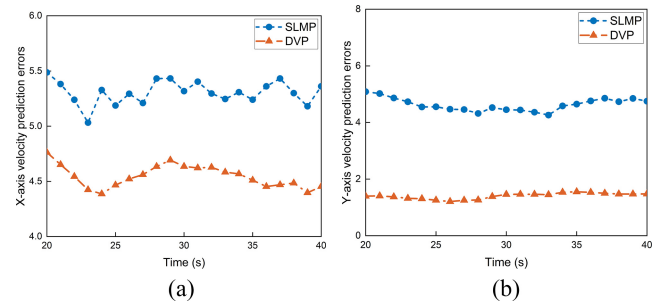


Fig. 8. Comparison of velocity prediction. (a) Comparison of X-axis velocity prediction. (b) Comparison of Y-axis velocity prediction.

TABLE III  
LOCATION PREDICTION

Algorithm	X-axis error	Y-axis error	Location error
<b>DVP</b>	0.0131	0.0045	0.00139
<b>SLMP</b>	0.0184	0.0068	0.00199
<b>Result</b>	-28.80%	-33.82%	-30.15%

node can predict its velocity and track its location based on the multistep LD algorithm. We will evaluate the velocity prediction algorithm by analyzing the velocity prediction error and location prediction error. First, the velocity prediction error in this article is compared with the velocity prediction error in the SLMP algorithm, which is denoted as DVP and SLMP, respectively. In Fig. 8, it can be seen that the velocity prediction of the algorithm on the  $X$ -axis and  $Y$ -axis is more accurate than that of the SLMP algorithm. The overall location prediction error is shown in Table III.

It can be found that the location prediction error of DVP is smaller than that of SLMP. This is because the velocity error will be amplified in the location prediction stage, and the accuracy of velocity prediction is the key to solving the problem of location prediction accuracy. Therefore, the DVP algorithm can obtain more accurate location prediction. It is worth noting that, if we solely depend on velocity prediction for estimating the location for the sensor node, the localization error will progressively increase. Therefore, when a certain time is reached, anchor node needs to obtain location and velocity information and rerun the DVP algorithm to maintain the accuracy of its velocity prediction.

3) *Results of Reference Nodes Optimization:* Four different schemes are simulated and compared to verify the influence of reference nodes optimization on positioning accuracy, including LSVP, random selection, SLMP, and ULES.

Simulation results show that the LSVP algorithm has good localization accuracy in the three scenarios of triangle deployment, grid deployment, and random deployment, especially in the scenario of random deployment of beacon nodes. This situation indicates that the reference nodes with different geometric relationships have a significant impact on localization accuracy, and selecting an appropriate reference node set can effectively improve the localization accuracy of network. From the three scenarios, we can observe that when the beacon

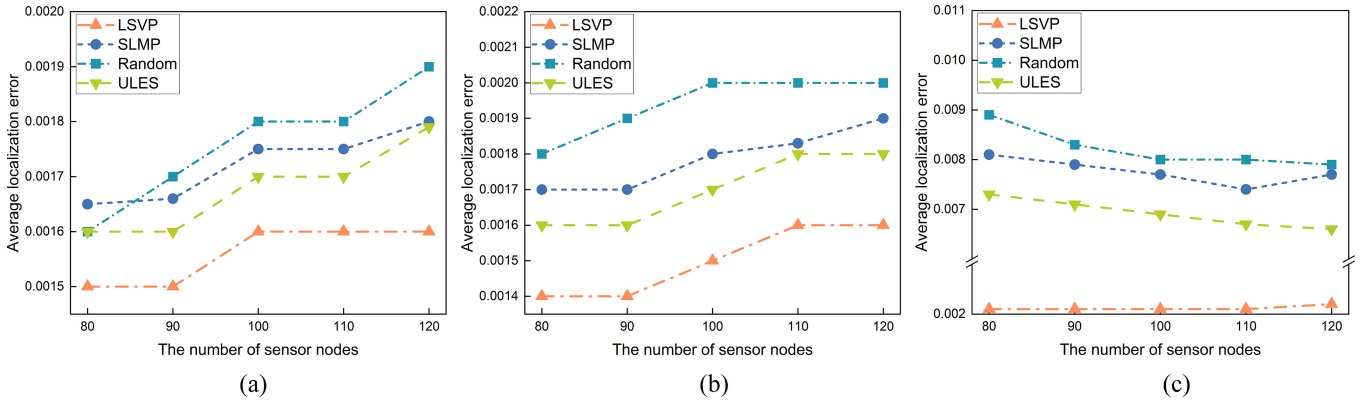


Fig. 9. Localization error versus the nodes' number. (a) Triangle deployment. (b) Grid deployment. (c) Random deployment.

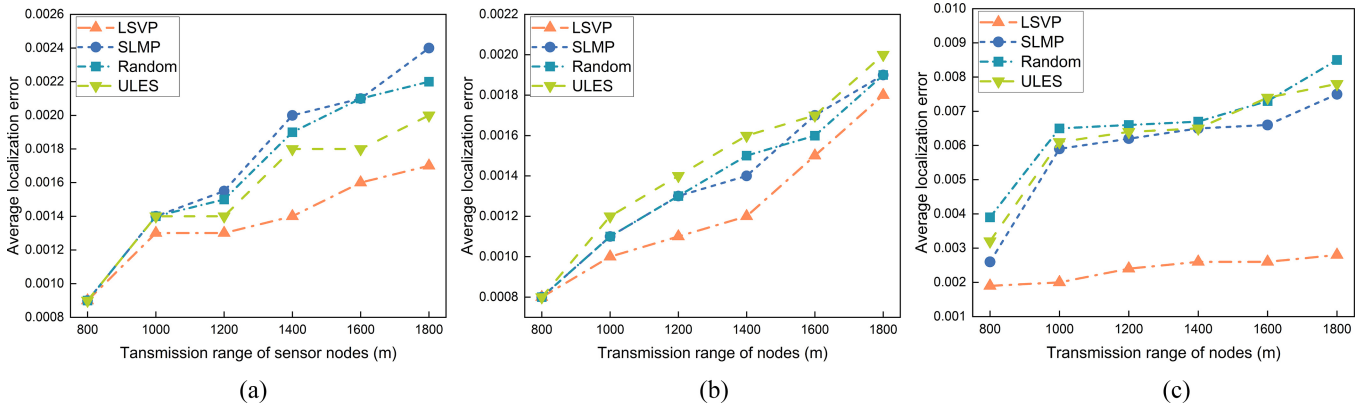


Fig. 10. Localization error versus transmission range. (a) Triangle deployment. (b) Grid deployment. (c) Random deployment.

nodes are distributed in triangle deployment, the ALE of all algorithms is smaller than those of the grid and random deployment. Because the triangle deployment of beacon nodes has a good geometric relationship. The reason why SLMP and Random perform slightly worse in the localization process without iteration is that both algorithms randomly select the reference node set.

In Fig. 9, we analyze the relationship between the ALE and the number of sensor nodes. The number of beacon nodes is 10, the number of other sensor nodes is from 80 to 120 and the iteration time is 1. As shown in Fig. 9, the ALE of LSVP is significantly lower than the other schemes, especially in the scenario of random deployment of beacon nodes. This is because the beacon nodes of triangle and grid deployment have regular geometric relationships, while the random deployment will bring large localization error without the reference node optimizations mechanism.

In Fig. 10, we show the relationship between the ALE and the transmission range of the sensor node. The number of sensor nodes was fixed at 120. In order to ignore the impact of error accumulation and error propagation, the number of localization iteration is set as 1. The sensor node communication range  $R_t$  is from 800 to 1800. The experimental results show that the ALE increases with the increase in the communication range. It should be noted that in the large-scale scenario of triangle and grid deployment, with the transmission range of sensor node being 800, the ALE of the four

algorithms is approximately the same. It is because, during the initial stage of the localization process, few beacon nodes are sparsely distributed in large-scale UASNs with wide spacing distance and small transmission range, making it difficult for unknown nodes to acquire enough reference nodes for localization. As there are only a few reference nodes, the reference node optimization mechanism in LSVP cannot be used to improve localization accuracy. But with the increment of the transmission range, LSVP has a lower ALE than other algorithms.

**4) Results of Iterative Localization:** In order to verify the effect of sensor node confidence calculation on reducing the ALE, we conducted a simulation comparison between LSVP, SLMP, and ULES, including the algorithm LSVP without  $\eta$  in this article (located nodes can be regarded as reference nodes directly in the iterative localization process). In Figs. 11 and 12, simulation results can verify the necessity of confidence value  $\eta$  and the good performance of the LSVP algorithm.

In Fig. 11, the number of sensor nodes is fixed as 120, and the communication range  $R_t$  of sensor nodes is 1800. It can be seen that the average localization errors increase with the increase of iteration times because with the increase of iteration times, cause more nonbeacon nodes are selected as reference nodes to assist the localization of other nodes. With the transmission and accumulation of errors, the ALE of the network gradually increases. Since there is no limitation of

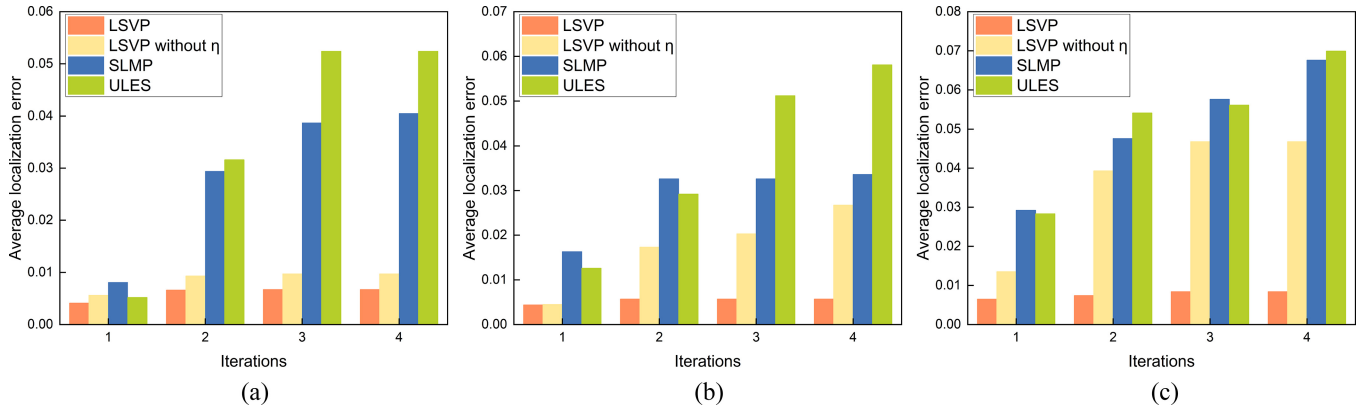


Fig. 11. Localization error versus the iteration times. (a) Triangle deployment. (b) Grid deployment. (c) Random deployment.

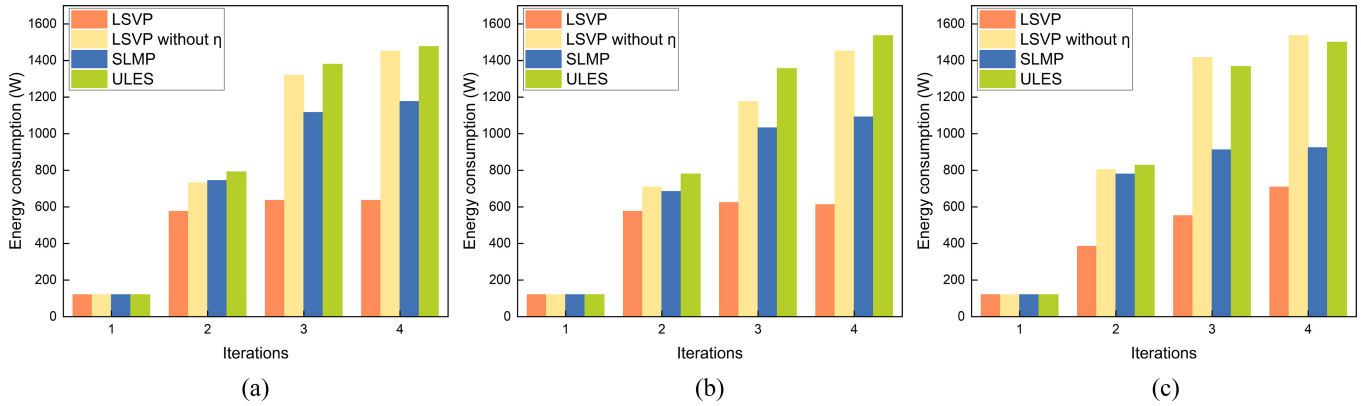


Fig. 12. Energy consumption versus the iteration times. (a) Triangle deployment. (b) Grid deployment. (c) Random deployment.

TABLE IV  
PROPORTION OF ALIVE SENSOR NODES DURING SIMULATION PERIODS

Algorithm	Triangle deployment				Grid deployment				Random deployment			
	100s	400s	700s	1000s	100s	400s	700s	1000s	100s	400s	700s	1000s
LSVP	100.00%	74.68%	50.77%	32.31%	100.00%	74.62%	54.62%	37.69%	100.00%	72.31%	49.23%	30.77%
SLMP	100.00%	73.14%	49.43%	29.23%	100.00%	73.08%	51.54%	30.77%	100.00%	79.23%	47.69%	28.46%
ULES	100.00%	68.53%	37.63%	12.31%	100.00%	65.39%	33.85%	10.00%	100.00%	66.15%	34.62%	10.00%

reference nodes during the execution of the ULES algorithm, any located node can serve as a pseudo-reference node, so the ALE is large. Despite LSVP without  $\eta$  having no limitation either, it still shows good performance on localization benefiting from the reference nodes optimization mechanism.

In Fig. 12, the number of sensor nodes is fixed as 120, and the communication range  $R_t$  of sensor nodes is 1800. Energy consumption increases with the increase of iteration times. This is because as the number of iteration increase, more located nodes can be used as pseudo-reference to assist other nodes in localization, which means more nodes will broadcast message. In the first iteration, only ten beacon nodes broadcast their information, resulting in the same energy consumption for the four algorithms. Since the SLMP algorithm suppresses the nodes which have poor localization results from

broadcasting data packets during the iterative localization, and on this basis, LSVP suppresses nodes with less energy from sending packets, the overall energy consumption of these two algorithms is low.

5) *Results of LSVP:* In order to verify the effectiveness of LSVP mechanism, we compare overall LSVP with SLMP and ULES algorithms. The overall energy efficiency advantage of LSVP algorithm was analyzed. A random initial energy is specified for each node, the communication energy consumption of sensor nodes is specified as 12 W, the iteration within a single localization period is specified as 3, the communication range is 1800 m, and the number of sensor nodes is specified as 120. We choose some specific times like 100, 400, 700, and 1000 s during the simulation time to show the survival ratio of each algorithm. Table IV shows the variation of node survival rate with simulation time under three scenarios.

As the localization algorithm progresses, the energy of nodes in the network is gradually consumed, and the number of surviving nodes in both three mechanisms decreases with the increase of the number of localization rounds. Compared with SLMP and ULES, LSVP has a higher percentage of node survival, because nodes with higher residual energy are more likely to serve as reference nodes in the process of localization. This mechanism prevents some nodes from consuming energy too fast, which can balance the energy consumption and prolong the lifetime of the entire network.

In general, the LSVP algorithm can significantly reduce the ALE and prolong the lifetime of the entire underwater sensor network.

## VI. CONCLUSION

This article proposes an efficient localization scheme LSVP for large-scale underwater sensor networks. In LSVP, both anchor node and ordinary node can complete real-time localization and location prediction. The moving pattern for anchor node is predicted based on the DVP algorithm, which can predict location with high accuracy and low energy consumption. And the CIL algorithm is designed for ordinary nodes to expand the localization coverage for large-scale underwater sensor networks, which can improve localization accuracy and alleviate error propagation. The simulation results show that LSVP can minimize the communication cost and prolong the NL while maintaining high-precision localization.

## REFERENCES

- [1] I. F. Akyildiz, D. Pompili, and T. Melodia, "Underwater acoustic sensor networks: Research challenges," *Ad Hoc Netw.*, vol. 3, no. 3, pp. 257–279, 2005.
- [2] S. N. Le, Y. Zhu, Z. Peng, J. Cui, and Z. Jiang, "PMAC: A real-world case study of underwater MAC," in *Proc. Conf. Underwater Netw. Syst. (WUWNet)*, 2013, pp. 1–8.
- [3] P. Xie, J. Cui, and L. Lao, "VBF: Vector-based forwarding protocol for underwater sensor networks," in *Proc. 5th Int. IFIP TC6 Netw. Technol., Services, Protocols; Perform. Comput. Commun. Netw.; Mobile Wireless Commun. Syst., Netw. Conf. ser.*, Coimbra, Portugal, 2006, pp. 1216–1221.
- [4] G. Tuna and V. C. Gungor, "A survey on deployment techniques, localization algorithms, and research challenges for underwater acoustic sensor networks," *Int. J. Commun. Syst.*, vol. 30, no. 17, p. e3350, 2017.
- [5] T. Bian, R. Venkatesan, and C. Li, "An improved Localization method using error probability distribution for underwater sensor networks," in *Proc. IEEE Int. Conf. Commun., ICC*, Cape Town, South Afr., May 2010, pp. 1–6.
- [6] A. Othman, A. E. Adams, and C. C. Tsimenidis, "Node discovery protocol and Localization for distributed underwater acoustic networks," in *Proc. Adv. Int. Conf. Telecommun. Int. Conf. Internet Web Appl. Services (AICT/ICIW 2006)*, Guadeloupe, French Caribbean, 2006, p. 93.
- [7] Z. Zhou, J. H. Cui, and S. Zhou, "Efficient localization for large-scale underwater sensor networks," *Ad Hoc Netw.*, vol. 8, no. 3, pp. 267–279, 2010.
- [8] Y. Su, L. Guo, Z. Jin, and X. Fu, "A mobile-beacon-based iterative Localization mechanism in large-scale underwater acoustic sensor networks," *IEEE Internet Things J.*, vol. 8, no. 5, pp. 3653–3664, Mar. 2021.
- [9] Z. Zhou, Z. Peng, J.-H. Cui, Z. Shi, and A. Bagtzoglou, "Scalable localization with mobility prediction for underwater sensor networks," *IEEE Trans. Mobile Comput.*, vol. 10, no. 3, pp. 335–348, Mar. 2011.
- [10] Y. Li, M. Liu, S. Zhang, R. Zheng, and J. Lan, "Node dynamic Localization and prediction algorithm for Internet of Underwater Things," *IEEE Internet Things J.*, vol. 9, no. 7, pp. 5380–5390, Apr. 2022.
- [11] J. Liu, Z. Wang, Z. Peng, J.-H. Cui, and L. Fiondella, "Suave: Swarm underwater autonomous vehicle localization," in *Proc. IEEE Conf. Comput. Commun., INFOCOM*, Toronto, Canada, 2014, pp. 64–72.
- [12] S. Lee and K. Kim, "Localization with a mobile beacon in underwater acoustic sensor networks," *Sensors*, vol. 12, no. 5, pp. 5486–5501, 2012.
- [13] V. Chandrasekhar and W. Seah, "An area localization scheme for underwater sensor networks," in *Proc. OCEANS 2006-Asia Pacific*, 2006, pp. 1–8.
- [14] X. Cheng, H. Shu, Q. Liang, and D. H.-C Du, "Silent positioning in underwater acoustic sensor networks," *IEEE Trans. Veh. Technol.*, vol. 57, no. 3, pp. 1756–1766, May 2008.
- [15] A. Y. Teymorian, W. Cheng, L. Ma, X. Cheng, X. Lu, and Z. Lu, "3D underwater sensor network Localization," *IEEE Trans. Mob. Comput.*, vol. 8, no. 12, pp. 1610–1621, Dec. 2009.
- [16] W. Cheng, A. Y. Teymorian, L. Ma, X. Cheng, X. Lu, and Z. Lu, "Underwater Localization in sparse 3D acoustic sensor networks," in *Proc. INFOCOM 2008. 27th IEEE Int. Conf. Comput. Commun., Joint Conf. IEEE Comput. Commun.*, Phoenix, AZ, USA, 2008, pp. 236–240.
- [17] B. Liu, H. Chen, Z. Zhong, and H. V. Poor, "Asymmetrical round trip based Synchronization-free Localization in large-scale underwater sensor networks," *IEEE Trans. Wirel. Commun.*, vol. 9, no. 11, pp. 3532–3542, Nov. 2010.
- [18] H. Chen, M. Liu, and S. Zhang, "Energy-efficient localization and target tracking via underwater mobile sensor networks," *Front. Inf. Technol. Electron. Eng.*, vol. 19, no. 8, pp. 999–1012, 2018.
- [19] J. Liu, Z. Wang, M. Zuba, Z. Peng, J. -H. Cui, and S. Zhou, "DA-sync: A doppler-assisted time-Synchronization scheme for mobile underwater sensor networks," *IEEE Trans. Mob. Comput.*, vol. 13, no. 3, pp. 582–595, Mar. 2014.
- [20] S. Song, J. Liu, J. Guo, C. Zhang, T. Yang, and J. Cui, "Efficient velocity estimation and location prediction in underwater acoustic sensor networks," *IEEE Internet Things J.*, vol. 9, no. 4, pp. 2984–2998, Feb. 2022.
- [21] A. C. Bagtzoglou and A. Novikov, "Chaotic Behavior and pollution dispersion characteristics in engineered tidal Embayments: A numerical investigation<sup>1</sup>," *JAWRA J. Amer. Water Resour. Assoc.*, vol. 43, no. 1, pp. 207–219, 2007.
- [22] P. Brockwell and R. Dahlhaus, "Generalized Levinson–Durbin and burg algorithms," *J. Econometrics*, vol. 118, nos. 1-2, pp. 129–149, 2004.
- [23] C. -H. Chen and K. -T. Feng, "Enhanced distance and location estimation for broadband wireless networks," *IEEE Trans. Mob. Comput.*, vol. 14, no. 11, pp. 2257–2271, Nov. 2015.
- [24] L. -C. Chu, P. -H. Tseng, and K. -T. Feng, "GDOP-assisted location estimation algorithms in wireless location systems," in *Proc. IEEE GLOBECOM 2008 - 2008 IEEE Global Commun. Conf.*, New Orleans, LA, USA, 2008, pp. 5404–5408.
- [25] N. Levanon, "Lowest GDOP in 2-D scenarios," *IEE Proc. Radar Sonar Navigation*, vol. 147, no. 3, pp. 149–155, 2000.
- [26] Z. Yang and Y. Liu, "Quality of trilateration: Confidence-based iterative Localization," *IEEE Trans. Parallel Distrib. Syst.*, vol. 21, no. 5, pp. 631–640, May 2010.
- [27] B. Huang, C. Yu, and B. D. O. Anderson, "Understanding error propagation in multihop sensor network localization," *IEEE Trans. Ind. Electron.*, vol. 60, no. 12, pp. 5811–5819, Dec. 2013.
- [28] N. H. Kussat, C. D. Chadwell, and R. Zimmerman, "Absolute positioning of an autonomous underwater vehicle using GPS and acoustic measurements," *IEEE J. Ocean. Eng.*, vol. 30, no. 1, pp. 153–164, Jan. 2005.
- [29] Z. Chen, Q. Hu, H. Li, R. Fan, and D. Ding, "ULES: Underwater Localization evaluation scheme under beacon node drift scenes," *IEEE Access*, vol. 6, pp. 70615–70624, 2018.



**Yiran Wang** received the B.S. and M.S. degrees in computer science and technology from Jilin University, Changchun, China, in 2017 and 2020, respectively, where she is currently pursuing the Ph.D. degree in computer application technology with the Department of Computer Science and Technology.

Her major research focuses on underwater localization and navigation.



**Shanshan Song** (Member, IEEE) received the B.S. and M.S. degrees in computer science and technology and the Ph.D. degree in management science and engineering from Jilin University, Changchun, China, in 2011, 2014, and 2018, respectively.

She was a Postdoctoral Researcher with the Department of Computer Science and Technology, Jilin University, where she is currently an Associate Professor. Her major research focuses on underwater data collection, localization and navigation, and machine learning.

Dr. Song serves as a reviewer for IEEE/ACM TRANSACTIONS ON NETWORKING, IEEE SENSORS JOURNAL, and *Future Generation Computer Systems*. She also serves as a TPC Member for the WUWNet'21 Conference, and a Session Chair for the ICCC'22 Conference.



**Qiang Ye** (Senior Member, IEEE) received the Ph.D. degree in electrical and computer engineering from the University of Waterloo, Waterloo, ON, Canada, in 2016.

Since September 2021, he has been an Assistant Professor with the Department of Computer Science, Memorial University of Newfoundland, St. John's, NL, Canada. Before joining Memorial, he was with the Department of Electrical and Computer Engineering and Technology, Minnesota State University, Mankato, MN, USA, as an Assistant Professor from September 2019 to August 2021 and the Department of Electrical and Computer Engineering, University of Waterloo as a Postdoctoral Fellow and then a Research Associate from December 2016 to September 2019. He has published over 55 research articles on top-ranked IEEE Journals and Conference Proceedings.

Dr. Ye is/was the General and a TPC Co-Chair for different international conferences and workshops, e.g., IEEE VTC'22, IEEE INFOCOM'22, and IEEE IPCCC'21. He serves/served as an Associate Editor for IEEE TRANSACTIONS ON COGNITIVE COMMUNICATIONS AND NETWORKING, IEEE OPEN JOURNAL OF THE COMMUNICATIONS SOCIETY, *Peer-to-Peer Networking and Applications*, *ACM/Wireless Networks*, and *International Journal of Distributed Sensor Networks*. He also serves as the IEEE Vehicular Technology Society (VTS) Regions 1–7 Chapters Coordinator from 2022 to 2023.



**Xiaoxin Guo** received the B.S., M.S., and Ph.D. degrees in computer science from the College of Computer Science and Technology, Jilin University, Changchun, China, in 1997, 2000, and 2005, respectively.

From 1999 to 2000, he worked as a full-time Software Engineer with North Technology Ltd., Sapporo, Japan. He was a Postdoctoral Fellow with the Montreal Neurological Institute, McGill University, Montreal, QC, Canada, from 2009 to 2010. Since 2000, he has been with the Key Laboratory of Symbol Computation and Knowledge Engineering of Ministry of Education, College of Computer Science and Technology, Jilin University, where he is currently a Professor. His research interests include computer vision, medical image processing, and computer graphics.



**Jun-Hong Cui** (Member, IEEE) received the B.S. degree in computer science from Jilin University, Changchun, China, in 1995, the M.S. degree in computer engineering from the Chinese Academy of Sciences, Guangzhou, China, in 1998, and the Ph.D. degree in computer science from the University of California at Los Angeles, Los Angeles, CA, USA, in 2003.

She was a Faculty with the Computer Science and Engineering Department, University of Connecticut, Mansfield, CT, USA. She is currently a Professor with the College of Computer Science and Technology, Jilin University, Changchun, China, and also with the Shenzhen Ocean Information Technology, Industry Research Institute, Shenzhen, China. Her research interests include the design, modeling, and performance evaluation of networks and distributed systems. Recently, her research mainly focuses on exploiting the spatial properties in the modeling of network topology, network mobility, and group membership, scalable and efficient communication support in overlay and peer-to-peer networks, and algorithm and protocol design in underwater sensor networks.

Prof. Cui is actively involved in the community as an organizer, a TPC member, and a reviewer for many conferences and journals. She is a Guest Editor for *ACM Mobile Computing and Communications Review* and *Ad Hoc Networks* (Elsevier). She co-founded the first ACM International Workshop on UnderWater Networks (WUWNet 2006) and currently serves as the WUWNet Steering Committee Chair. She is a member of ACM, ACM SIGCOMM, ACM SIGMOBILE, IEEE Computer Society, and IEEE Communications Society.



**Jun Liu** (Member, IEEE) received the B.Eng. degree in computer science from Wuhan University, Wuhan, China, in 2002, and the Ph.D. degree in computer science and engineering from the University of Connecticut, Mansfield, CT, USA, in 2013.

He is currently a Professor with the School of Electronic and Information Engineering, Beihang University, Beijing, China, also a part-time Professor with the Robotics Research Center, Peng Cheng Laboratory, Shenzhen, China. His major research focuses on underwater acoustic networking, time synchronization, localization, network deployment, and also interested in operating system and cross-layer design.

Prof. Liu is a member of the IEEE Computer Society.